

# <sup>1</sup> MotilA – A Python pipeline for the analysis of microglial fine process motility in 3D time-lapse multiphoton microscopy data

<sup>4</sup> **Fabrizio Musacchio**  <sup>1</sup>¶, **Sophie Crux**<sup>1</sup>, **Felix Nebeling**<sup>1</sup>, **Nala Gockel**<sup>1</sup>, **Falko Fuhrmann**<sup>1</sup>, and **Martin Fuhrmann**  <sup>1</sup>

<sup>6</sup> 1 German Center for Neurodegenerative Diseases (DZNE), Bonn, Germany ¶ Corresponding author

DOI: [10.xxxxxx/draft](https://doi.org/10.xxxxxx/draft)

## Software

- [Review](#) 
- [Repository](#) 
- [Archive](#) 

---

Editor: [Open Journals](#) 

Reviewers:

- [@openjournals](#)

Submitted: 01 January 1970

Published: unpublished

## License

Authors of papers retain copyright and release the work under a Creative Commons Attribution 4.0 International License ([CC BY 4.0](#)).<sup>17</sup>

## <sup>7</sup> Summary

<sup>8</sup> *MotilA* is an open-source Python pipeline for quantifying microglial fine-process motility in <sup>9</sup> 3D time-lapse two-channel fluorescence microscopy. It was developed for high-resolution <sup>10</sup> *in vivo* multiphoton imaging and supports single-stack and batch analyses. The workflow <sup>11</sup> performs sub-volume extraction, optional registration/unmixing, z-projection, segmentation, <sup>12</sup> and pixel-wise change detection to compute the turnover rate (TOR). The code is platform <sup>13</sup> independent, documented with tutorials and example datasets, and released under GPL-3.0.

## <sup>14</sup> Statement of need

<sup>15</sup> Microglia are immune cells of the central nervous system and continuously remodel processes <sup>16</sup> to survey brain tissue and respond to pathology ([M. Fuhrmann et al., 2010](#); [Nimmerjahn et al., 2005](#); [Prinz et al., 2019](#); [Tremblay et al., 2010](#)). Quantifying this subcellular motility is <sup>17</sup> important for studies of neuroinflammation, neurodegeneration, and synaptic plasticity. Current <sup>18</sup> practice in many labs relies on manual or semi-manual measurements in general-purpose tools <sup>19</sup> such as Fiji/ImageJ or proprietary software ([Carl Zeiss Microscopy GmbH, Accessed 2025](#); <sup>20</sup> [Schindelin et al., 2012](#)). These procedures are time consuming, hard to reproduce, focus on <sup>21</sup> single cells, and are sensitive to user bias. ([Brown, 2017](#); [Wall et al., 2018](#)). There is no <sup>22</sup> dedicated, open, and batch-capable solution tailored to this task. <sup>23</sup>

<sup>24</sup> *MotilA* fills this gap with an end-to-end, reproducible pipeline for 3D time-lapse two-channel <sup>25</sup> imaging. It standardizes preprocessing, segmentation, and motility quantification and scales <sup>26</sup> from individual stacks to large experimental cohorts. Although optimized for microglia, the <sup>27</sup> approach generalizes to other motile structures that can be reliably segmented over time. <sup>28</sup>

## <sup>28</sup> Implementation and core method

<sup>29</sup> Input is a 5D stack in TZCYX or TZYX order, where T is time, Z is depth, C is channel, <sup>30</sup> and YX are spatial dimensions. For each time point, *MotilA* extracts a user-defined z-sub- <sup>31</sup> volume, optionally performs 3D motion correction and spectral unmixing, and computes a 2D <sup>32</sup> maximum-intensity projection to enable interpretable segmentation. After thresholding, the <sup>33</sup> binarized projection  $B(t_i)$  is compared with  $B(t_{i+1})$  to derive a change map

$$\Delta B(t_i) = 2B(t_i) - B(t_{i+1}).$$

<sup>34</sup> Pixels are classified as stable “S” ( $\Delta B = 1$ ), gained “G” ( $\Delta B = -1$ ), or lost “L” ( $\Delta B = 2$ ). <sup>35</sup> From these counts, the turnover rate is defined as

$$TOR = \frac{G + L}{S + G + L},$$

representing the fraction of pixels that changed between consecutive frames. This pixel-based strategy follows earlier microglial motility work (M. Fuhrmann et al., 2010; Nebeling et al., 2023) while providing a fully automated and batchable implementation with parameter logging and diagnostics.

The pipeline exposes options for 3D or 2D registration, contrast-limited adaptive histogram equalization, histogram matching across time to mitigate bleaching, and median or Gaussian filtering (Pizer et al., 1987; Virtanen et al., 2020; Walt et al., 2014). Results include segmented images, G/L/S/TOR values, brightness and area traces, and spreadsheets for downstream statistics. Memory-efficient reading and chunked processing of large TIFFs are supported via Zarr (Miles et al., 2025).

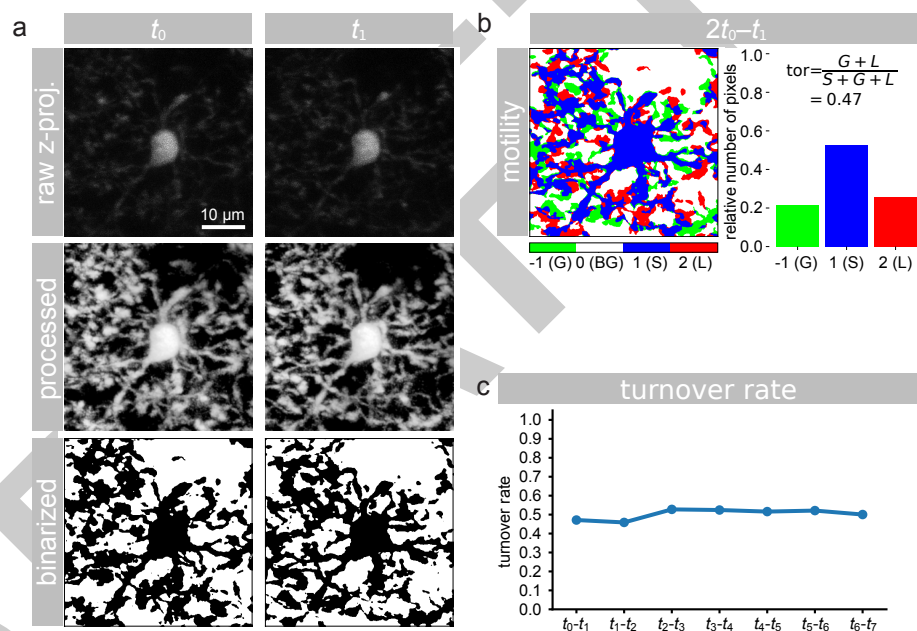


**Figure 1:** Example analysis with MotilA. a) z-projected microglial images at two consecutive time points ( $t_0$ ,  $t_1$ ), shown as raw, processed, and binarized data. b) pixel-wise classification of gained (G), stable (S), and lost (L) pixels used to compute the turnover rate (TOR). c) TOR values across time points from the same dataset, illustrating dynamic remodeling of microglial fine processes.

## 46 Usage

MotilA can be called from Python scripts or Jupyter notebooks. Three entry points cover common scenarios: process\_stack for a single stack, batch\_process\_stacks for a project folder organized by dataset identifiers with a shared metadata sheet, and batch\_collect to aggregate metrics across datasets. All steps write intermediate outputs and logs to facilitate validation and reproducibility. MotilA's GitHub repository provides tutorials and an example dataset to shorten onboarding.

## 53 Applications and scope

MotilA has been applied to quantify microglial process dynamics in several *in vivo* imaging studies and preprints (Crux et al., 2024; F. Fuhrmann et al., 2024; Gockel et al., 2025). Typical use cases include baseline surveillance behavior, responses to neuroinflammation or genetic

57 perturbations, and deep three-photon imaging where manual analysis is impractical. The  
58 binarize-and-compare principle can in principle be adapted to other structures such as dendrites  
59 or axons when segmentation across time is robust.

## 60 Limitations

61 Using 2D projections simplifies processing but sacrifices axial specificity and can merge  
62 overlapping structures. Segmentation quality determines accuracy and can be affected by  
63 vessels, low signal-to-noise ratios, or strong intensity drift. The current spectral unmixing is a  
64 simple subtraction; advanced approaches may be needed for some fluorophores. *MotilA* targets  
65 pixel-level process motility rather than object-level tracking or full morphometry.

## 66 Example dataset

67 The repository includes two *in vivo* two-photon stacks from mouse frontal cortex formatted for  
68 use with *MotilA* (Gockel et al., 2025). Each stack contains eight time points at five-minute  
69 intervals, two channels for microglia and neurons, and approximately sixty z-planes at one  
70 micrometer steps in a field of view of about 125 by 125 micrometers. The example reproduces  
71 the full analysis, including projections, segmentation, change maps, brightness traces, and  
72 TOR over time, and serves as a template for cohort-level workflows.

## 73 Availability

74 Source code, documentation, tutorials, and issue tracking are hosted at: <https://github.com/FabrizioMusacchio/motila>. The software runs on Windows, macOS, and Linux with Python 3.9  
75 or newer and standard scientific Python stacks. It is released under GPL-3.0, and contributions  
76 via pull requests or issues are welcome.  
77

## 78 Acknowledgements

79 We thank the Light Microscopy Facility and Animal Research Facility at the DZNE, Bonn, for  
80 essential support. This work was supported by the DZNE and grants to MF from the ERC  
81 (MicroSynCom 865618) and the DFG (SFB1089 C01, B06; SPP2395). MF is a member of  
82 the DFG Excellence Cluster ImmunoSensation2. Additional support came from the iBehave  
83 network and the CANTAR network funded by the Ministry of Culture and Science of North  
84 Rhine-Westphalia, and from the Mildred-Scheel School of Oncology Cologne-Bonn. Animal  
85 procedures followed institutional and national regulations, with efforts to reduce numbers and  
86 refine conditions.

## 87 References

- 88 Brown, D. L. (2017). Bias in image analysis and its solution: Unbiased stereology. *Journal of Toxicologic Pathology*, 30(3), 183–191. <https://doi.org/10.1293/tox.2017-0013>
- 89 Carl Zeiss Microscopy GmbH. (Accessed 2025). *ZEISS ZEN Microscopy Software*. <https://www.zeiss.com.metrology/en/software/zeiss-zen-core.html>.
- 90 Crux, S., Roggan, M. D., Poll, S., Nebeling, F. C., Schiweck, J., Mittag, M., Musacchio, F.,  
91 Steffen, J., Wolff, K. M., Baral, A., Witke, W., Gurniak, C., Bradke, F., & Fuhrmann,  
92 M. (2024). Deficiency of actin depolymerizing factors ADF/Cfl1 in microglia decreases  
93 motility and impairs memory. *bioRxiv*. <https://doi.org/10.1101/2024.09.27.615114>
- 94 Fuhrmann, F., Nebeling, F. C., Musacchio, F., Mittag, M., Poll, S., Müller, M., Giovannetti, E.  
95 A., Maibach, M., Schaffran, B., Burnside, E., Chan, I. C. W., Lagurin, A. S., Reichenbach,  
96 N., Kaushalya, S., Fried, H., Linden, S., Petzold, G. C., Tavosanis, G., Bradke, F., &  
97 Fuhrmann, M. (2024). Three-photon *in vivo* imaging of neurons and glia in the medial

- 100 prefrontal cortex with sub-cellular resolution. *bioRxiv*. <https://doi.org/10.1101/2024.08.28.610026>
- 101
- 102 Fuhrmann, M., Bittner, T., Jung, C. K. E., Burgold, S., Page, R. M., Mitteregger, G., Haass, C., LaFerla, F. M., Kretzschmar, H., & Herms, J. (2010). Microglial Cx3cr1 knockout prevents neuron loss in a mouse model of alzheimer's disease. *Nature Neuroscience*, 13(4), 411–413. <https://doi.org/10.1038/nn.2511>
- 103
- 104
- 105
- 106 Gockel, N., Nieves-Rivera, N., Druart, M., Jaako, K., Fuhrmann, F., Rožkalne, R., Musacchio, F., Poll, S., Jansone, B., Fuhrmann, M., & Magueresse, C. L. (2025). *Example datasets for microglial motility analysis using the MotilA pipeline*. Zenodo. <https://doi.org/10.5281/zenodo.15061566>
- 107
- 108
- 109
- 110 Miles, A., jakirkham, Hamman, J., Orfanos, D. P., Stansby, D., Bussonnier, M., Moore, J., Bennett, D., Augspurger, T., Rzepka, N., Cherian, D., Verma, S., Bourbeau, J., Fulton, A., Abernathey, R., Lee, G., Spitz, H., Kristensen, M. R. B., Jones, M., & Schut, V. (2025). *Zarr-developers/zarr-python: v3.0.6* (Version v3.0.6). Zenodo. <https://doi.org/10.5281/zenodo.3773449>
- 111
- 112
- 113
- 114
- 115 Nebeling, F. C., Poll, S., Justus, L. C., Steffen, J., Keppler, K., Mittag, M., & Fuhrmann, M. (2023). Microglial motility is modulated by neuronal activity and correlates with dendritic spine plasticity in the hippocampus of awake mice. *eLife*, 12, e83176. <https://doi.org/10.7554/eLife.83176>
- 116
- 117
- 118
- 119 Nimmerjahn, A., Kirchhoff, F., & Helmchen, F. (2005). Resting microglial cells are highly dynamic surveillants of brain parenchyma in vivo. *Science*, 308(5726), 1314–1318. <https://doi.org/10.1126/science.1110647>
- 120
- 121
- 122 Pizer, S. M., Amburn, E. P., Austin, J. D., Cromartie, R., Geselowitz, A., Greer, T., Haar Romeny, B. ter, Zimmerman, J. B., & Zuiderveld, K. (1987). Adaptive histogram equalization and its variations. *Computer Vision, Graphics, and Image Processing*, 39(3), 355–368. [https://doi.org/10.1016/S0734-189X\(87\)80186-X](https://doi.org/10.1016/S0734-189X(87)80186-X)
- 123
- 124
- 125
- 126 Prinz, M., Jung, S., & Priller, J. (2019). Microglia biology: One century of evolving concepts. *Cell*, 179(2), 292–311. <https://doi.org/10.1016/j.cell.2019.08.053>
- 127
- 128 Schindelin, J., Arganda-Carreras, I., Frise, E., Kaynig, V., Longair, M., Pietzsch, T., Preibisch, S., Rueden, C., Saalfeld, S., Schmid, B., & others. (2012). Fiji: An open-source platform for biological-image analysis. *Nature Methods*, 9(7), 676–682. <https://doi.org/10.1038/nmeth.2019>
- 129
- 130
- 131
- 132 Tremblay, M.-È., Lowery, R. L., & Majewska, A. K. (2010). Microglial interactions with synapses are modulated by visual experience. *PLOS Biology*, 8(11), 1–16. <https://doi.org/10.1371/journal.pbio.1000527>
- 133
- 134
- 135 Virtanen, P., Gommers, R., Oliphant, T. E., Haberland, M., Reddy, T., Cournapeau, D., Burovski, E., Peterson, P., Weckesser, W., Bright, J., Walt, S. J. van der, Brett, M., Wilson, J., Millman, K. J., Mayorov, N., Nelson, A. R. J., Jones, E., Kern, R., Larson, E., ... Contributors, S. 1.0. (2020). SciPy 1.0: Fundamental algorithms for scientific computing in python. *Nature Methods*, 17, 261–272. <https://doi.org/10.1038/s41592-019-0686-2>
- 136
- 137
- 138
- 139
- 140 Wall, E., Blaha, L. M., Paul, C. L., Cook, K., & Endert, A. (2018). Four perspectives on human bias in visual analytics. In G. Ellis (Ed.), *Cognitive biases in visualizations* (pp. 29–42). Springer International Publishing. [https://doi.org/10.1007/978-3-319-95831-6\\_3](https://doi.org/10.1007/978-3-319-95831-6_3)
- 141
- 142
- 143 Walt, S. van der, Schönberger, J. L., Nunez-Iglesias, J., Boulogne, F., Warner, J. D., Yager, N., Gouillart, E., Yu, T., & contributors, the scikit-image. (2014). Scikit-image: Image processing in python. *PeerJ*, 2, e453. <https://doi.org/10.7717/peerj.453>
- 144
- 145